

Remote Visualization and Computational Steering of Cardiac Virtual Tissues using gViz

OV Aslanidi¹, KW Brodli², RH Clayton³, JW Handley², AV Holden¹, J Wood²

¹Computational Biology Laboratory, School of Biomedical Sciences, University of Leeds, Leeds LS2 9JT

²School of Computing, University of Leeds, Leeds, LS2 9JT

³Department of Computer Science, University of Sheffield, Sheffield S1 4DP

Abstract

Cardiac tissue engineering - detailed biophysical, histological and anatomical models of the heart - is moving from developmental research projects towards high throughput applications. This emerging immense computational load can be reduced by computational steering, and realised via visualization on remote grid or high end compute resources. We illustrate a solution using a library of computational steering middleware (gViz), to control simulations of the effects of low voltage approaches to defibrillation.

1. Introduction

Cardiovascular disease is the single most common cause of premature adult deaths in the Western industrialised world. Atrial flutter/fibrillation is a common precursor of cerebral stroke, and ventricular fibrillation a common cause of death. Over half of the mortality from cardiovascular disease is due to sudden cardiac deaths, occurring within 24 hours of a cardiac event. Ventricular fibrillation (VF) is recorded in about three quarters of sudden cardiac deaths victims reached promptly by emergency paramedics [1, 2].

During VF the synchronized, mechanical pumping action of the ventricles is lost, and irregular trembling of the ventricular muscle is produced by irregular excitation, which manifest as a high frequency, irregular electrocardiogram. Clinical, experimental and theoretical studies all suggest that VF can be produced by re-entrant propagation of a number of moving, interacting rotors within the ventricle. Computational models within an anatomically detailed ventricular geometry [3] allowed plausible simulations [4-6] of how an intraventricular scroll wave can break down into a fluctuating number of interacting re-entrant waves. Fig. 1 shows some examples of these behaviours.

Virtual ventricular tissues are anatomically and biophysically detailed computational models of ventricular tissues. They have proved to be an effective tool for simulating normal and abnormal ventricular propagation patterns, and for proposing hypotheses that can be tested experimentally [4-8].

Cardiac tissue is electrically excitable and supports travelling waves of electrical

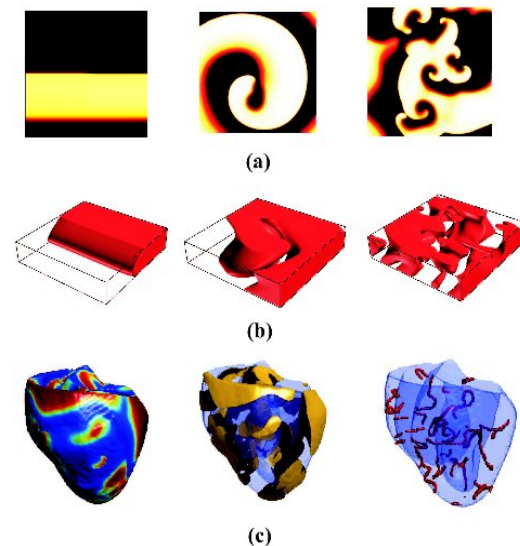


Fig. 1. Examples of normal and re-entrant propagation in virtual cardiac tissues. (a) Propagation of a plane wave (left), single re-entrant wave (middle), and multiple re-entrant waves (right) in 150 x 150mm 2D model. (b) Snapshots of a plane wave (left), single scroll wave (middle), and multiple scroll waves (right) in a 3D anisotropic model of cardiac tissue with dimensions of 82 x 82 x 16 mm. Red regions are isosurfaces enclosing regions of active tissue. (c) Snapshots of membrane voltage on the heart surface (left), membrane voltage isosurfaces (middle), and filaments (right) during simulated VF in the canine ventricle.

excitation. Dynamics of the excitation, primarily the membrane potential, V (mV), of cardiac cells forming the tissue, can be described by the nonlinear reaction-diffusion partial differential equation (PDE) [6, 9]:

$$\frac{\partial V}{\partial t} = \nabla(D\nabla V) - I_{\text{ion}} \quad (1)$$

Here ∇ is a spatial gradient operator; t is time (ms); D is the effective diffusion coefficient; a tensor in 3D, ($\text{mm}^2 \text{ms}^{-1}$), that characterizes electrotonic spread of voltage, primarily through the intercellular gap junctions; I_{ion} is the total membrane ionic current ($\mu\text{A } \mu\text{F}^{-1}$).

A number of different models of cardiac cell electrophysiology have been developed, so the voltage and time dependent current I_{ion} can be specified for different species and for different regions of the heart [10]. Here we use the high-order, biophysically detailed Luo-Rudy (LRd) family [11] of ventricular cell models, and a simplification, the Fenton-Karma (FK) family of models [12].

A key biomedical problem is how re-entrant arrhythmias develop and can be controlled. The vulnerability of cardiac virtual tissue to re-entry can be measured by the width of the vulnerable window (VW), in time or space, which is the range of intervals (or spatial extent) where a localised S2 excitation of appropriate amplitude and duration in the wake of a propagating wave initiated by a spatially remote S1 stimulus can lead to uni-directional conduction block in 1-D or re-entry in 2-D. This can be estimated using 1-D homogenous/heterogeneous PDE models, and the development and control of re-entry can be followed in 2-D models.

While virtual cells forming models of 1- and 2-D tissues can be run on a single CPU, 3-D tissues are more suitable for SMP parallel computation [13]. A "virtual heartbeat" - around 1 second of simulated activity in the human heart - requires about 10^{14} floating point operations. Current pharmacological and bioengineering applications demand high throughput, while prospective patient-specific clinical applications require high bandwidth access from tertiary clinical centres to teraflop compute resources. Computational steering of simulations run on Grid or remote High End Computing Centres provides a cost-effective solution that is available with current technologies.

2. Computational Steering

The concept of computational steering is outlined by Marshall et al. [14] where they identify three approaches to the visualization of output from a simulation. First, a simple *post-processing* approach where the simulation is run first, and the results later visualized. This is the typical approach used by most computational scientists and has an advantage that results can be examined in depth, at the scientist's own pace, and different visualization techniques used. The second approach is *tracking*, in which

images are viewed as the calculation proceeds, allowing errors to be spotted and fruitless calculations aborted. The scientist can interact with the visualization to control the view that is taken. The third approach is *steering*, where the scientist interacts with both the simulation and the visualization.

While the first model is straightforward, for the second two the gViz library [15-17] was developed. When linked into simulation code it allows users to connect to running simulations from suitably augmented client software and receive computed data for visualization and deliver parameters for steering using a simple API. In this way, a simulation can appear to be running on the user's desktop, with all the interactivity and control that affords, when it is in fact running on a Grid resource, with the associated computing power. The library is essentially a communications tool between clients and simulations to enable this. Furthermore, once a client/simulation approach

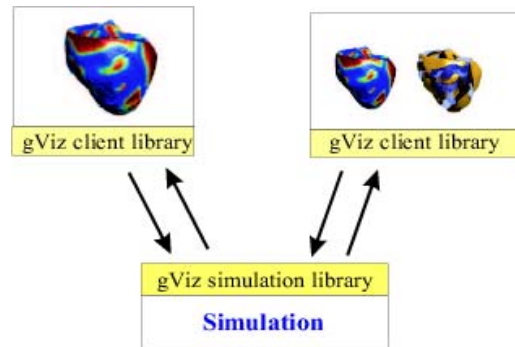


Fig. 2. Architecture of the gViz steering library: two client applications (at different locations) connect to a simulation with communication handled by the gViz library.

is adopted, it becomes possible for more than one user to observe and interact with a given simulation, raising the possibility of collaborative visualization and steering. Figure 2 gives an overview of the gViz architecture, showing two clients connected to a single simulation of cardiac virtual tissue.

This mechanism has been used to monitor the progress of many simple heart model simulations as well as being used to computationally steer more complex re-entrant spiral wave problems. The gViz library was developed in the e-Science Core Programme project on Visualization Middleware. The work reported here describes the further evolution and application of the gViz middleware within the e-Science Pilot Project on Integrative Biology (<http://www.integrativebiology.ac.uk>), and the EPSRC-funded project on An Advanced Environment to Enable Visual Supercomputing (e-Viz). A key aspect of the Integrative Biology project is providing the computational infrastructure for the study of heart diseases.

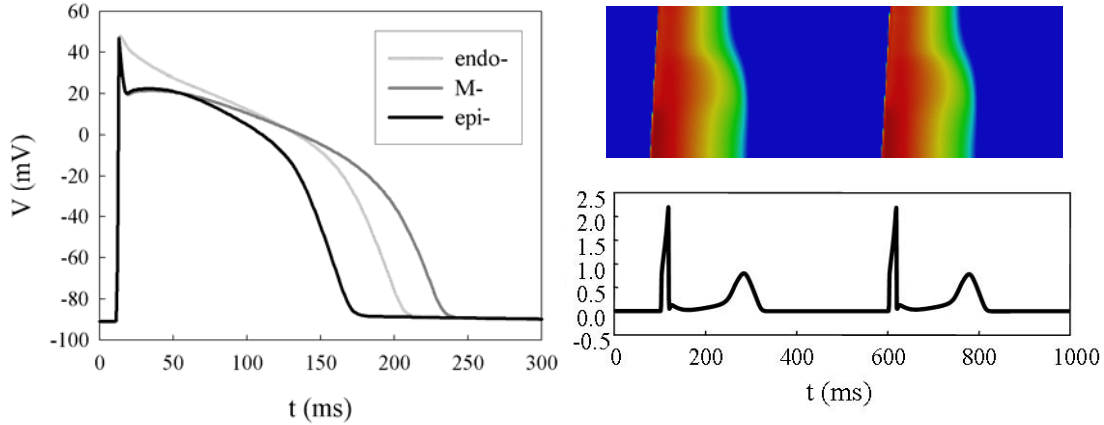


Fig. 3. Solitary wave propagation in the virtual ventricular wall consisting of three compact regions (endo-, M- and epi-), each occupying a third of the 15 mm wall. Cellular action potentials (left) are shown along with space-time plots of the membrane voltage (top right) colour-coded using a rainbow palette. The wall is repetitively stimulated from the endocardial end leading to the upward wave propagation. Pseudo-ECG (bottom right) generated by the spatial membrane voltage distribution within the wall is estimated using the standard expression [18].

3. Vulnerability in 1-D

The equation (1) in one dimension has a spatially uniform solution, corresponding to the resting tissue, and can support solitary wave propagation. Fig. 3 illustrates propagation of excitation waves through the 1D virtual ventricular wall with transmural differences, i.e. consisting of endo-, M- and epicardial cells [18]. One-dimensional models can be useful for studying pathologies that affect transmural propagation patterns, and can be detected from changes at electrocardiograms (ECGs) [18, 19].

The VW in physical space defines where unidirectional conduction block and re-entrant propagation can be initiated by a localized suprathreshold (in terms of spatial extent, current intensity and duration) excitation, that may be an applied stimulus, or an ectopic excitation.

The VW for a heterogeneous (ventricular transmural) strand is illustrated in Fig 4. The VW, and its dependence on membrane parameters that are modified to reproduce pharmacological actions, or the effects of genetic mutations, is obtained from families of stimulations at each parameter set, and so mapping the vulnerable window requires extensive batch mode solution of PDEs in parameter space. The VW is small (a few milliseconds, compared to action potential durations of a few hundred milliseconds and beat-beat intervals of the order of seconds). Typically a ‘brute force’ approach is taken, where the entire parameter space is searched for each VW. If such simulations are monitored at run-time, however, unfruitful simulations can be terminated early, saving compute cycles. Furthermore, on-line visual tracking of the

solutions allows the boundaries of the VW, rather than the interior and exterior, to be mapped. S2 excitation parameter selection based on the VW boundaries for neighbouring excitation parameter values, allows continuation of the VW boundaries in physical or parameter

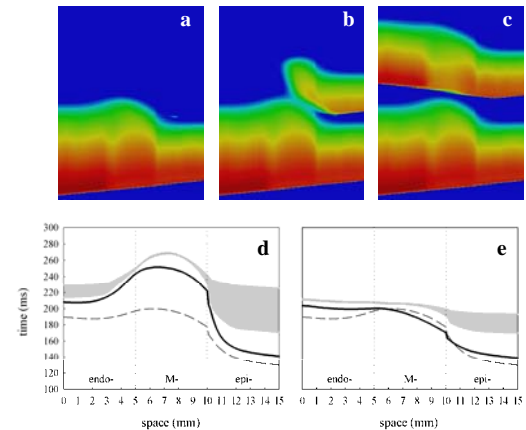


Fig. 4. Transmural AP propagation and VW definition in the virtual ventricular wall. The wall is stimulated from the endocardial end (at the left), leading to the AP propagation. Further S2 stimulation with different timing results in either (a) propagation failure, (b) unidirectional block or (c) bidirectional propagation. Space-time plots are shown, the membrane voltage is colour-coded using the standard rainbow palette. Each panel presents 400 ms of activity in 15 mm thick wall. Effects of (d) d-sotalol and (e) amiodarone on the virtual wall: spatial distributions of APD through the normal wall (dashed line) and the wall treated by the drugs (solid lines) are shown along with the respective VWs (grey areas).

space. Together these can reduce the computational load by around two orders of magnitude.

4. Re-entry in 2-D

A re-entrant spiral wave solution appears as a circulation of excitation, around the core, which acts as an organizing centre that imposes its rhythm on the rest of the tissue by emitting propagating waves. In both experimental observations and in numerical investigations with homogeneous, isotropic tissues spiral waves need not rotate rigidly, around a circular core, but can meander. In meander the tip of the spiral wave (defined in experiments by a phase singularity, or the point on a voltage isoline where the wavefront meets the waveback, and in numerical solutions by intersection of isolines of two state variables, say voltage and a gating variable) can follow a complicated trajectory. Enhanced meander, or induced drift, of the spiral wave so that it reaches a boundary of the medium provides a means of extinguishing re-entrant activity that has been proposed as an explanation for self-terminating ventricular tachyarrhythmias, and as a means of low-voltage defibrillation.

One method uses local control of a global perturbation to produce resonant drift [20].

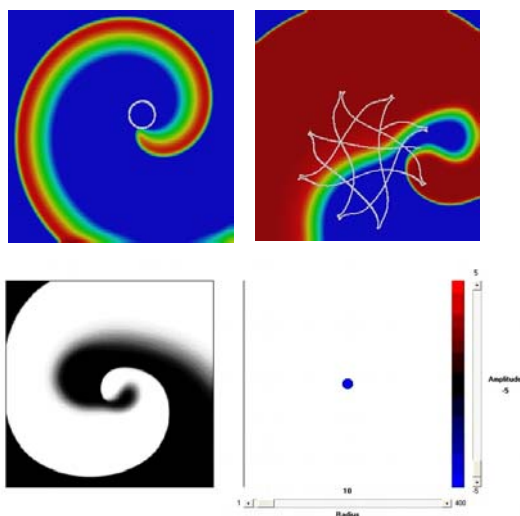


Fig. 5. Illustration of re-entry. Top: Re-entrant spiral waves in 2D isotropic homogeneous virtual ventricular tissue with the Fenton-Karma excitation kinetics. Spatial distribution of the membrane voltage is colour-coded using a rainbow palette. Depending on the parameters, the tip trajectories show either rigid rotation (left) or extended meander (right). Bottom: Screenshot of the steering client. The left panel shows the current simulation output (greyscale colour-coded membrane voltage), with the right side showing the current stimulus settings. Stimuli are applied by clicking on the appropriate location in the left panel.

However, the response functions of a spiral wave (a measure of sensitivity to perturbation) are nonzero only in the vicinity of the tip of the spiral [21], and so a perturbation localized to the tip would require a much lower energy to eliminate re-entry; the “defibrillation threshold energy” would be lower by the ratio of the core/filament area/volume to the medium area/volume. The inclusion of gViz in such a simulation allows for experimentation into the effect of localized perturbations on the spiral wave. Perturbations of varying amplitude, area of coverage, and location may be applied to the simulation as it runs, with immediately visible results. Alternatively, pathologies or pharmacologies of varying strength/composition can be introduced at simulation time, and the effect these have on subsequent perturbations examined. This enables large parameter spaces to be rapidly explored by identifying and expanding fruitful lines of research and ignoring ‘dead-ends’, as opposed to having to schedule a large number of batch jobs and post-process the results. By using computationally simplified models on high performance compute resources, ‘coarse’ results are immediately obtained that may be refined by running more detailed or accurate models using parameters identified in the coarse experiments.

5. Implementation

The Fenton-Karma model provides a simplified description of the total membrane ionic current, but reproduces the rapid upstroke velocity, overall shape and restitution properties of ventricular action potentials. We use the Fenton-Karma model with parameters given in Table 1 of the original paper [12] to produce the action potential duration (APD) and conduction velocity restitution of the modified Beeler-Reuter (MBR) model for ventricular cells. The equation (1) is solved on a 400 x 400 spatial grid using a finite-difference PDE solver that implements the explicit Euler method with time and space steps $\Delta t = 0.10$ ms and $\Delta x = 0.20$ mm, respectively. The PDE solver was parallelized under OpenMP and run on 16 UltraSparcIII processors of a local SunFire 6800 machine.

The gViz library was linked into the above simulation by adding the gViz API calls to output simulation data and to update the simulation parameters based on any steering. The data output by the simulation were the membrane potential at every cell, and current simulation time. The parameters used in the steering were an (x,y) location, radius, and amplitude of a stimulus to apply. The client was developed in Matlab using gVizMatlab – a set of routines that enable Matlab to communicate with a gViz enabled simulation. This client was run under Windows XP, and an example screenshot is shown in Fig. 5.

6. Results and Discussion

We have illustrated the use of both computational tracking and steering of cardiac virtual tissues, in the context of evaluating pro-arrhythmic actions of actual anti-arrhythmics, and in evaluating low voltage approaches to defibrillation. These applications not only allow an increase in efficiency, but also remote, thin client, computational steering of HPC resources.

The use of gViz allowed interactive tracking of cores of moving spiral waves, and run-time simulation within the cores. Applying a series of negative stimuli in the path of a moving core enabled drift and elimination of the spiral wave at the boundary of the tissue (Fig. 6). Thus, in this case computational steering provides a method for “defibrillation” of the virtual tissue by accurately timed low-amplitude electrical intervention. On the other hand, positive stimulation of the core in our simulations never resulted in elimination of the spirals: their cores either merged with the stimuli, demonstrating usual patterns of meander, or were destroyed by the interaction with it, resulting in breakdown of the spiral (Fig. 6, bottom). Hence, our computations can also be used for finding a boundary between anti- and pro-arrhythmic effects of the stimulation.

Note that it is possible to algorithmically identify the spiral wave core, and hence this analysis would have been possible using the traditional post-processing approach. However, every variation in timing, location, amplitude, or radius of the stimuli – however small – would entail re-programming or re-scripting the simulation, running it again and post-processing the results. On the other hand, computational steering allowed for instant variation and evaluation of stimuli application, while also removing the need to develop the code to apply the stimuli. Additionally, while algorithmically locating the spiral wave core is straightforward in the case of a single spiral wave in a homogeneous domain, once multiple spiral waves or heterogeneous domains are considered the problem is much harder. Computational steering allows the human operator to make these decisions at run-time.

These methods are available as a tool for prescreening of putative anti-arrhythmics (as in the European Union NoE BioSim: <http://chaos.fys.dtu.dk/biosim/index.jsp>) and the evaluation of cardiac defibrillation and pacing algorithms. If the parametric intervention is a change in excitation rate coefficients (to simulate the effects of local cooling) or the diffusion coefficient (to simulate the effects of ablation) these methods are readily applicable to heterogeneous models of endocardial surface activity, and allow patient specific prediction of the effects of reversible, cryological or irreversible, surgical ablations.

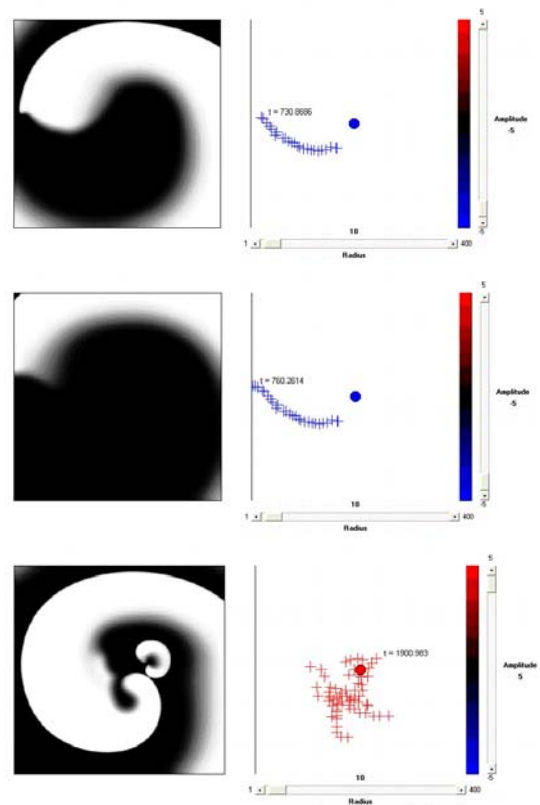


Fig. 6. Computational steering of 2D Fenton-Karma virtual ventricular tissue. A series of negative stimuli forces a spiral wave to drift to the tissue boundary (top, middle), whereas positive stimulation breaks the spiral down (bottom). Screenshots of the steering client are shown as before, with the simulation output on the left and the stimuli control and history on the right.

7. Conclusion

The use of gViz with cardiac virtual tissue enables the rapid exploration of parameter space, with the associated potential for both discovery and more efficient usage of computational resources. These advantages become more important as the computational complexity increases, and the models move to patient specific 3D models. In addition to this, when a model of a patient’s physiology has been built, it is not hard to imagine the scenario of a clinician and a pharmacologist wishing to collaboratively interact with the running model in order to establish the best routine of care for that patient, a scenario that gViz enables through remote visualization and computational steering of patient specific cardiac virtual tissues.

Acknowledgements

We would like to acknowledge the EPSRC funding support for this work, through the following projects: GR/R96231/01 - Visualization Middleware for e-Science; GR/S4658/01 - An Advanced Environment to Enable Visual Supercomputing; GR/S72023/01 - e-Science Pilot Project on Integrative Biology, and the EU - Biosim NoE 005137.

References

- [1] Huikuri, H.V., Castellanos, A., Myerburg, R.J. Sudden death due to cardiac arrhythmias. *N. Engl. J. Med.* 345 (2001), 1473-1482.
- [2] Priori, S.G., Aliot, E., Blomstrom-Lundqvist, C. et al. Update of the guidelines on sudden cardiac death of the European Society of Cardiology. *Eur. Heart. J.* 24 (2003), 13-15.
- [3] Nielsen, P.M.F., LeGrice, I.J.E., Smaill, B.H., Hunter, P.J. Mathematical model of geometry and fibrous structure of the heart. *Am. J. Physiol.* 29 (1991), H1365-H1378.
- [4] Panfilov, A.V., Keener J.P. Re-entry in an anatomical model of the heart. *Chaos Solitons & Fractals* 5 (1995), 681-699.
- [5] Berenfeld, O., Jalife J. Purkinje-muscle reentry as a mechanism of polymorphic ventricular arrhythmias in a 3-dimensional model of the ventricles. *Circ. Res.* 82 (1998), 1063-1077.
- [6] Clayton, R.H., Holden, A.V. Filament behavior in a computational model of ventricular fibrillation in the canine heart. *IEEE Trans. Biomed. Eng.* 51 (2004), 28-34.
- [7] Biktashev, V.N., Holden, A.V., Mironov, S.F., Pertsov, A.M., Zaitsev, A.V. Three-dimensional aspects of re-entry in experimental and numerical models of ventricular fibrillation. *Int. J. Bifurcation & Chaos* 9 (1999), 695-704.
- [8] Xie, F., Qu, Z., Yang, J., Baher, A., Weiss, J.N., Garfinkel, A. A simulation study of the effects of cardiac anatomy in ventricular fibrillation. *J. Clin. Invest.* 113 (2004), 686-693.
- [9] Clayton, R.H., Holden, A.V. Computational framework for simulating the mechanisms and ECG of re-entrant ventricular fibrillation. *Physiol. Meas.* 23 (2002), 707-726.
- [10] Noble, D., Rudy, Y. Models of cardiac ventricular action potentials: iterative interaction between experiment and simulation. *Phil. Trans. Royal Soc. London* A359 (2001), 1127-1142.
- [11] Luo, C.H., Rudy Y. A dynamic model of the cardiac ventricular action potential. I. Simulations of ionic currents and concentration changes. *Circ. Res.* 74 (1994), 1071-1096.
- [12] Fenton, F., Karma, A. Vortex dynamics in three-dimensional continuous myocardium with fibre rotation: Filament instability and fibrillation. *Chaos* 8 (1998), 20-47.
- [13] Clayton, R.H., Holden, A.V. Virtual tissue engineering of the heart. *Int. J. Bifurcation and Chaos* 13 (2003), 3531-3886.
- [14] Marshall, R., Kempf, S., Dyer, S., Yen, C. Visualization methods and simulations steering for a 3D turbulence model for Lake Erie. *SIGGRAPH Computer Graphics* 24 (1990), pp. 89-97.
- [15] Wood, J., Brodlie, K., Walton, J. g-Viz: Visualization and steering on the Grid. *Proc. UK e-Science All Hands Meeting 2003*, EPSRC.
- [16] Brodlie, K., Wood, J., Duce, D., Sagar, M. gViz: Visualization and computational steering on the Grid. *Proc. UK e-Science All Hands Meeting 2004*, EPSRC.
- [17] Brodlie, K., Duce, D., Gallop, J., Sagar, M., Walton, J., Wood, J. Visualization in Grid Computing Environments. *Proceedings of IEEE Visualization 2004*, edited by H. Rushmeier, G. Turk and J.J. van Wijk, pp. 155-162. ISBN: 0-7803-8788-0 (2004).
- [18] Gima, K., Rudy Y. Ionic current basis of electrocardiographic waveforms – a model study. *Circ. Res.* 90 (2002), 889-896.
- [19] Aslanidi, O.V., Clayton, R.H., Lambert, J.L., Holden, A.V. Dynamical and cellular electrophysiological mechanisms of ECG changes during ischaemia. *J. Theor. Biol.* (2005), in press.
- [20] Biktashev, V.N., Holden, A.V. Re-entrant arrhythmias and their control in models of ventricular tissue. *J. Electrocardiology* 32 (1999), 76-83.
- [21] Biktasheva, I.V., Biktashev, V.N. On a wave-particle dualism of spiral wave dynamics. *Phys. Rev. E* 67 (2003), 26221.